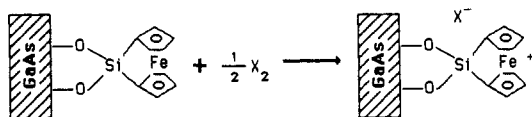


Figure 1. Uncorrected PL spectra of a derivatized n-GaAs sample before (solid line) and after (dotted line) treatment with I_2 vapor in flowing N_2 . Following the reaction with I_2 , treatment with gaseous N_2H_4 regenerates the solid curve. The sample was excited with the 457.9-nm line of an Ar^+ laser.

Scheme I



Excitation of the derivatized sample with ultraband gap 457.9-nm light ($E_g \sim 1.4$ eV) in an atmosphere of N_2 produces edge emission at 865 nm, as shown in Figure 1. No change in the PL spectrum is observed when the sample is subsequently exposed to H_2 , O_2 , CO , CH_4 , and H_2O vapor. However, introduction of a volatile oxidant such as I_2 by sublimation in a flow of N_2 produces rapid quenching of the PL intensity; within a few seconds, the limiting 40% quenching shown in the figure is reached. A slightly greater degree of quenching is observed with dry, gaseous Br_2 .⁶ That quenching corresponds to oxidation of the ferrocene derivative, as shown in Scheme I, is supported by the restoration of the original PL signal by chemical or electrochemical reduction. In the former case, the gaseous reductant N_2H_4 rapidly reverses the effect of I_2 ; the PL changes were reversible during 10 cycles of alternate exposure to I_2 and N_2H_4 .⁷ Alternatively, use of the I_2 -treated sample as an electrode evidences the expected ferricenium dark reduction wave at -0.25 V vs. SCE in the aforementioned electrolyte, concomitant with the return of PL quenching by gaseous I_2 . In control experiments, PL from n-GaAs samples that were either only etched or etched and treated with $(CH_3)_2SiCl_2$ showed no effect upon exposure to I_2 , dry Br_2 , or N_2H_4 .

The PL spectral changes induced by I_2 are indicative of an expansion in the electric field in the semiconductor; on electrostatic grounds, such an effect is consistent with the presence of negatively charged (poly)halide ions near the semiconductor surface, as shown in Scheme I. By regarding the region supporting the electric field as being completely nonemissive, i.e., a dead layer, a quantitative expression for relative PL intensity is obtained, eq 1; this treatment

$$\Delta D = \frac{-\ln(PL_{ox}/PL_{red})}{\alpha'} \quad (1)$$

assumes that the n-GaAs surface recombination velocity is either very large or insensitive to the oxidant.⁸ In eq 1, PL_{red} and PL_{ox} are the PL intensities before and after the addition of the oxidant, ΔD is the corresponding change in dead-layer thickness, and α'

$= (\alpha + \beta)$ with α and β the solid's absorptivities for the exciting and emitted light. A quantitative test of the dead-layer model is the calculation of a constant value for ΔD using several interrogating wavelengths of varying optical penetration depth. We find that the PL quenching observed with 457.9-, 514.5-, and 632.8-nm excitation yields, using literature absorptivities,⁹ a consistent value for ΔD of 260 Å. The satisfactory accord with the dead-layer model is consistent with an electrostatic origin of PL quenching. Alternatively, the quenching may reflect the shift in the redox potential of the surface monolayers; a concomitant shift in the semiconductor's Fermi level would also produce these PL effects.

In summary, chemistry occurring within a few monolayers can modulate the electric field thickness of an underlying semiconductor by several hundred angstroms, producing corresponding variations in PL intensity. This coupling of a molecular species to a semiconductor substrate represents a general contactless method for monitoring changes in surface chemistry. Furthermore, by exploiting molecular reactivity patterns, semiconductor/molecular interfaces with targeted chemical specificity can be designed for use as optically coupled sensors.

Acknowledgment. We are grateful to the Office of Naval Research, the Army Research Office, and the 3M Co. for generous support of this research. We thank Dr. Alan C. Thomas for experimental assistance and a reviewer for helpful comments.

Registry No. I_2 , 7553-56-2; Br_2 , 7726-95-6; N_2H_4 , 302-01-2.

(9) An absorptivity of 4.35×10^4 cm^{-1} at 632.8 nm was interpolated from: Sturge, M. D. *Phys. Rev.* **1962**, *127*, 768. Absorptivities of 9.38×10^4 and 1.99×10^5 cm^{-1} were used at 514.5 and 457.9 nm, respectively; these values were obtained via dead-layer analysis of PL quenching from samples operating in photoelectrochemical cells: Burk, A. A., Jr.; Johnson, P. B.; Hobson, W. S.; Ellis, A. B. *J. Appl. Phys.* **1986**, *59*, 1621.

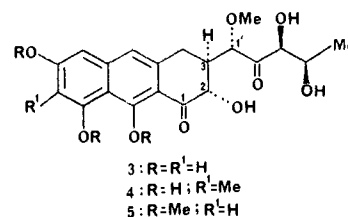
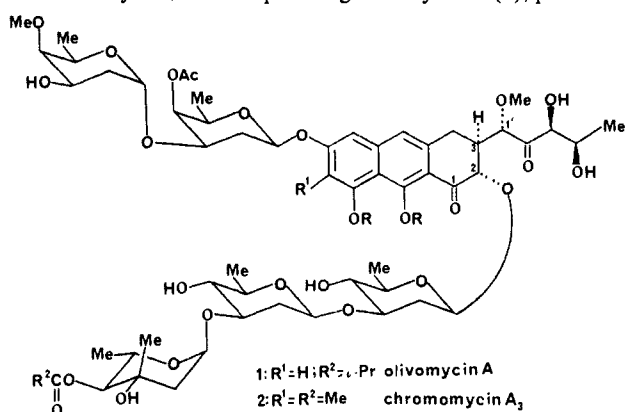
Stereoselective Total Synthesis of the Natural Enantiomer of Olivin Trimethyl Ether

R. W. Franck,* V. Bhat, and C. S. Subramaniam

Chemistry Department, Hunter College/CUNY
New York, New York 10021

Received November 29, 1985

The olivomycins, an example being olivomycin A (1), produced



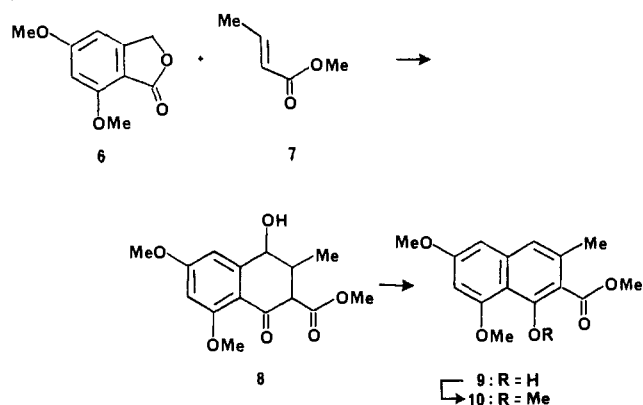
by *Streptomyces olivoreticuli*, belong to the aureolic acid family

(6) Water vapor had no effect upon the I_2 -initiated quenching (and restoration of PL with N_2H_4), but trace amounts of water present in the gaseous Br_2 led to etching of the surface.

(7) PL from derivatized samples stored in either oxidation state under Ar at -10 °C for a week remained sensitive to redox chemistry, although the magnitude of the effect diminished by a few percent.

(8) Hobson, W. S.; Ellis, A. B. *J. Appl. Phys.* **1983**, *54*, 5956.

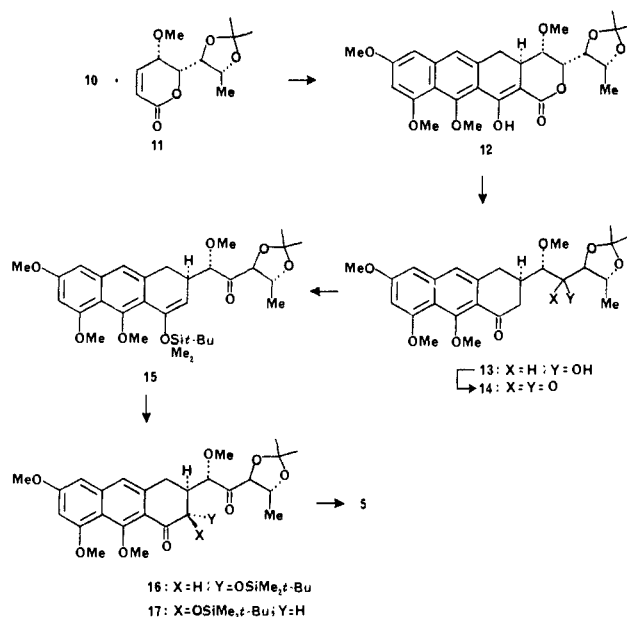
Scheme I



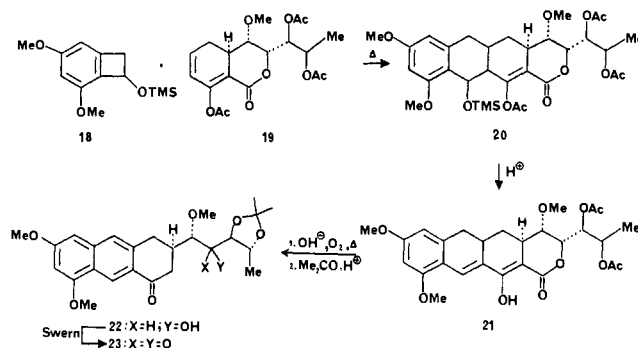
of antitumor antibiotics along with mithramycin (aureolic acid) and the chromomycins (e.g., **2**).¹ These compounds have seen limited clinical use in cancer chemotherapy. Their aglycones, olivin (**3**) and chromomycinone (**4**), have been synthetic targets for organic chemists² and, recently, Weinreb and co-workers^{2f} have reported the first total synthesis of tri-*O*-methylolivin (**5**) in its racemic form. In this paper, we wish to describe our efforts which have produced the first stereoselective total synthesis of **5** in its natural form. It is also significant that our synthesis is the first to unambiguously confirm the stereochemistry assigned to the aglycone.

Condensation of 5,7-dimethoxyphthalide (**6**)³ with methyl crotonate (**7**) (LDA, DME, -78°C to room temperature) gave the hydroxytetralone intermediate **8** which, without purification, was directly aromatized to provide the naphthol **9**, mp $85\text{--}86^{\circ}\text{C}$, in 52% overall yield from **6**.⁴ Methylation of the naphthol **9** ($(\text{CH}_3)_2\text{SO}_4$, K_2CO_3 , acetone, reflux) resulted in the naphthoate **10**, mp $95\text{--}96^{\circ}\text{C}$ in 91% yield (Scheme I). Michael–Claisen condensation of **10** with the unsaturated lactone **11**⁵ (LDA, THF-DMPU⁶, -78°C) gave after an aqueous workup, the tetracyclic intermediate **12** which, without purification, was directly saponified and decarboxylated (0.05 N aqueous NaOH, EtOH, 75°C , 5 h) to give the hydroxy anthracenone **13** as a single stereoisomer ($[\alpha]_{\text{D}} + 6.43^{\circ}$, c 0.28, CHCl_3), in 51% yield starting from **10**. Swern oxidation⁷ of **13** (Me_2SO , TFAA, Et_3N , CH_2Cl_2 , -60°C) furnished the diketone **14** ($[\alpha]_{\text{D}} - 13^{\circ}$, c 0.31, CHCl_3) in 85% yield. To complete the total synthesis of **5**, there remained only the introduction of the hydroxyl function at C-2 and the deprotection of the side chain isopropylidene moiety. Toward this end, the diketone **14** was chemoselectively converted to the enol silyl ether **15**, employing the conditions reported by Mander and Sethi⁸ (TBDMS triflate, Et_3N , CH_2Cl_2 , room temperature, 15 min). Without purification, **15** was immediately subjected to oxidation (*m*-CPBA, 1,2-dichloroethane, -15°C to room temperature)⁹ to give, after chromatography, mainly the silylated

Scheme II



Scheme III



trans-acyloin **16** (67.5%) along with 8.5% of the *cis* isomer **17**. Finally, hydrolysis of **16** (Dowex H⁺, 50W-X8, MeOH, room temperature 24 h) furnished **5** (95%) (Scheme II), as a gum which had identical TLC, 400-MHz NMR, and CD [λ_{max} (MeOH) 302 ($\Delta\epsilon$ 1.28) and 335 nm ($\Delta\epsilon$ -0.82)] with the gummy material obtained from degradation of **1** [$\text{CD } \lambda_{\text{max}}$ (MeOH) 302 ($\Delta\epsilon$ 1.36) and 334 nm ($\Delta\epsilon$ -1.04)].¹⁰

The key stereochemical feature of our work is the establishment of the C-3 configuration in the Michael–Claisen merger of **10** and **11** to form **12**. There is precedent, largely from the field of prostaglandin synthesis¹¹ for conjugate addition to cyclic enones from the face opposite an allylic alkoxy group. Thus, we were confident of the relative and absolute configuration drawn in **12–17**. To reinforce our belief, we carried out the sequence shown in Scheme III, where the synthon **19** was derived from material whose stereochemistry was established by X-ray crystallography.^{2e} In the event, anthracenones **22** and **23** gave ¹H NMR spectra (400 MHz) that were essentially identical with those of **13** and **14** (except for an extra methoxyl group in **13** and **14** in place of the aromatic hydrogens in **22** and **23**). It is interesting to note that the relative configuration at C-3 and C-1' of the natural aglycones

(1) Remers, W. A. *The Chemistry of Antitumor Antibiotics*; Wiley: New York, 1979; Vol. 1, and references cited therein.

(2) (a) Dodd, J. H.; Garigipati, R. S.; Weinreb, S. M. *J. Org. Chem.* **1982**, *47*, 4045. (b) Franck, R. W.; John, T. V. *J. Org. Chem.* **1983**, *48*, 3269. (c) Kraus, G. A.; Hagen, M. D. *J. Org. Chem.* **1983**, *48*, 3265. (d) Datta, S. C.; Franck, R. W.; Noire, P. D. *J. Org. Chem.* **1984**, *49*, 2785. (e) Franck, R. W.; Subramaniam, C. S.; John, T. V.; Blount, J. F. *Tetrahedron Lett.* **1984**, 2439. (f) Dodd, J. H.; Starrett, J. E.; Weinreb, S. M. *J. Am. Chem. Soc.* **1984**, *106*, 1811. (g) Roush, W. R.; Harris, D. J.; Lesur, B. M. *Tetrahedron Lett.* **1983**, 2227. (h) Thiem, J.; Wessel, H. P. *Liebigs Ann. Chem.* **1981**, 2216.

(3) Noire, P. D.; Franck, R. W. *Synthesis* **1980**, 882 and references cited therein.

(4) Broom, N. J. P.; Sammes, P. G. *J. Chem. Soc., Perkin Trans. 1* **1981**, 465. (b) Hauser, F. M.; Rhee, R. P. *J. Org. Chem.* **1977**, *42*, 4155.

(5) The lactone **11** ($[\alpha]_{\text{D}} + 198.3^{\circ}$, c 22.3, CHCl_3) was obtained from commercially available *D*-fucose through a seven-step sequence in an overall yield of 43% (see ref 2e).

(6) DMPU = *N,N'*-dimethylpropyleneurea: see, Mukhopadhyay, T.; Seebach, D. *Helv. Chim. Acta* **1982**, *65*, 385.

(7) Omura, K.; Sharma, A. K.; Swern, D. *J. Org. Chem.* **1976**, *41*, 957.

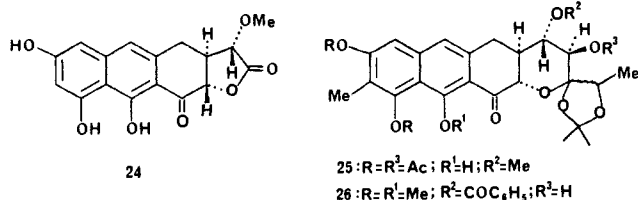
(8) Mander, L. N.; Sethi, S. P. *Tetrahedron Lett.* **1984**, 5953.

(9) (a) Rubottom, G. M.; Vazquez, M. A.; Pelegrina, D. R. *Tetrahedron Lett.* **1974**, 4319. (b) Hassner, A.; Reuss, R. H.; Pinnick, H. W. *J. Org. Chem.* **1975**, *40*, 3427. (c) Jones, T. K.; Denmark, S. E. *J. Org. Chem.* **1985**, *50*, 4037.

(10) Olivomycin A (**1**) was first subjected to acid hydrolysis (0.1 N MeOH/ H_2SO_4 , reflux, 3 h) to provide **3**, which was then methylated (CH_2N_2 , $\text{Et}_2\text{O}/\text{THF}$, room temperature 12 h) to afford **5**.

(11) (a) Binns, M. R.; Haynes, R. K.; Lambert, D. E.; Schober, P. A. *Tetrahedron Lett.* **1985**, 3385 and references cited therein. (b) Rosen, T.; Taschner, M. J.; Thomas, J. A.; Heathcock, C. H. *J. Org. Chem.* **1985**, *50*, 1190. (c) Nemoto, H.; Nagai, M.; Fukumoto, K.; Kametani, T. *Tetrahedron* **1985**, *41*, 2361.

had been assigned by NMR studies of degradation product **24**



for olivin¹² and studies of cyclic bis-ketal **25**, a derivative of a potassium carbonate catalyzed rearrangement product of chromomycinone.¹³ The absolute configuration at C-1' in olivin was based on a CD comparison with D-O-methyl mandelic ester; while in chromomycinone, a benzoate **26** obtained from **25** was subject to an early interpretation of Davydov splitting in the CD (exciton chirality rule).¹⁴ Hence, we believe that our synthesis using a known sugar and stereoselective chemistry confirms the assignments of relative and absolute configuration of olivin **3**.¹⁵

Acknowledgment. We are indebted to the National Cancer Institute for Grant CA 37359, which supported the work. The JEOL GX 400 NMR spectrometer used in this work was purchased with funds awarded by NSF-PCM 111745. We are grateful to Professor S. M. Weinreb for several helpful discussions, for making available unpublished experimental details of his work, for supplying comparison spectra, and for a gift of olivomycin A for use in the degradation to obtain authentic trimethylolivin.

(12) Bakhaeva, G. P.; Berlin, Y. A.; Chuprunova, O. A.; Kolosov, M. N.; Peck, G. Y.; Piotrovich, L. A.; Schemyakin, M. M.; Vasina, I. V. *J. Chem. Soc., Chem. Commun.* **1967**, 10.

(13) Miyamoto, M.; Morita, K.; Kawamatsu, Y.; Kawashima, K.; Nakanishi, K. *Tetrahedron* **1967**, 23, 411.

(14) Harada, N.; Nakanishi, K.; Tatsuoka, S. *J. Am. Chem. Soc.* **1969**, 91, 5896.

(15) The structure assigned to each new compound was in accord with its infrared and 400-MHz ¹H NMR spectra. The key intermediates **9**, **13** (derivatized as its trimethylsilyl ether), and **16** were also analyzed by their high-resolution mass spectra.

C₆₀La: A Deflated Soccer Ball?

D. M. Cox,* D. J. Trevor, K. C. Reichmann, and A. Kaldor

Corporate Research, Exxon Research and Engineering Co., Annandale, New Jersey 08801

Received January 30, 1986

A recent paper by Heath et al.¹ (HOZLCKTS) reported very exciting results; the production and detection of C_nLa complexes, n = 44, 46, 48, ..., 76, with n = 60 the dominant species. For the dominant C_nLa species, C₆₀La, the metal atom was postulated, on the basis of the experimental photoionization mass spectroscopy data, to be strongly bound within a spheroidal carbon shell possessing unusually high stability. In this paper we present further experimental evidence which when added to the information presented by HOZLCKTS and Kroto et al.² (KHOCS) seriously challenges this enticing conclusion.

Three experimental observations compelled HOZLCKTS to confidently propose this novel structure. First, KHOCS reported that C₆₀ was the most intense bare cluster ion observed in the photoionization mass spectra (PMS) of bare carbon clusters; second, when a lanthanum-impregnated graphite substrate was vaporized, C₆₀La was the most intense C_nLa lanthanum-containing cluster ion; third, only C_nLa complexes containing one lanthanum atom were detected in the PMS.

(1) Heath, J. R.; O'Brien, S. C.; Zhang, Q.; Liu, Y.; Curl, R. F.; Kroto, H. W.; Tittel, F. K.; Smalley, R. E. *J. Am. Chem. Soc.* **1985**, 107, 7779-7780.

(2) Kroto, H. W.; Heath, J. R.; O'Brien, S. C.; Curl, R. F.; Smalley, R. E. *Nature (London)* **1985**, 318, 162-163.

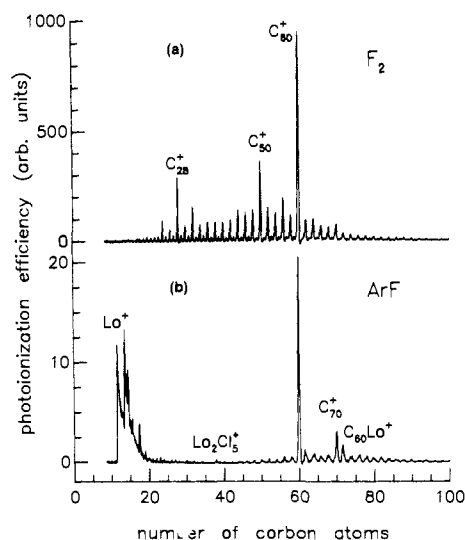


Figure 1. Photoionization time of flight mass spectra obtained from pulsed-laser vaporization of a lanthanum-impregnated graphite rod is shown for (a) ionization by F₂ and (b) ionization by ArF. The lower panel (b) was obtained when unfocused ArF (6.42-eV photons, 1.17 mJ/pulse) was the ionizing laser while the upper panel (a) was obtained when unfocused F₂ (7.87-eV photons, 0.05 mJ/pulse) was the ionizing laser. Except for the fact that the multiplier gain was reduced a factor of 2.6 for (a), all other experimental parameters were identical. The ionizing laser beam was collimated by a 0.125 cm high by 1.0 cm long slit. The vaporization laser intensity was ~360 MW/cm² (28 mJ at 532 nm of which ~50% was focused to a 1-mm-diameter spot on the lanthanum-impregnated graphite rod). The cluster source geometry simply consisted of the pulsed nozzle operated with 10 atm of helium backing pressure. The helium pulses pass through a 0.1-cm-diameter tube. At the graphite rod located 0.5 cm from the nozzle exit, this tube opens up to 0.2-cm diameter for a length of 4.5 cm before exiting to vacuum.

In addition to confirming the above experimental observations, we have found that (a) all C_nLa⁺ have ionization thresholds below 6.42 eV, the ArF photon energy, whereas, under identical conditions, bare C_n, n = 40-100, have ionization thresholds above 6.42 eV,⁴ (b) all C_n and C_nLa clusters for n = 44-76 have ionization thresholds below 7.87 eV, the F₂ photon energy, and (c) the photoionization efficiency (ions produced per unit photon flux) for C_n⁺ is 2 orders of magnitude larger when ionizing with 7.87-eV photons than it is with 6.42-eV photons, whereas it is only a factor of 2-4 larger for C_nLa⁺. Such effects significantly alter the magnitude of the C_n⁺ signals relative to the C_nLa⁺ signals and, if not taken into account, can lead to erroneous conclusions regarding the relative abundance of the corresponding neutral parent species.

The lower trace in Figure 1 shows the time of flight mass spectrum obtained for ionization with 6.42 eV (ArF). For the clusters containing 40-80 atoms, Figure 1b is in all respects quite similar to that published by HOZLCKTS. The most intense peaks are C₆₀⁺, C₇₀⁺, and C₆₀La⁺. The weaker peaks are C_{n-12}La⁺, 5 amu to the low-mass side of C_n⁺. The upper trace was obtained under identical operating conditions except that the ionization was with 7.87-eV photons with substantially less photon flux (see figure caption for details). The major difference between Figure 1, parts a and b, in the 40-80 cluster size range is that in Figure 1b the peaks (except for C₆₀⁺ and C₇₀⁺) are C_nLa⁺, whereas in Figure

(3) Only results for even atom clusters are discussed here.

(4) Cox, D. M.; Trevor, D. J.; Reichmann, K. C.; Kaldor, A., unpublished results. This paper will detail our results for bare C_n clusters. We find that the large variations in the C₆₀ ion signal can be understood as an interplay between large changes in photoionization efficiency and fragmentation pathways dependent upon ionizing laser frequency and intensity. The C₆₀⁺ signal exhibits a complex dependence on ArF ionizing laser intensity, which depends upon the specific experimental conditions. It exhibits either a linear or a quadratic dependence on the ArF ionizing laser intensity dependent upon the ionizing laser intensity, the vaporizing laser intensity, and/or the length of a 2-mm diameter extender tube through which the evaporated material must pass.